Final Draft
of the original manuscript:

Gebhard, S.; Pyczak, F.; Goeken, M.:
Microstructural and micromechanical characterisation of TiAl alloys using atomic force microscopy and nanoindentation
In: Materials Science and Engineering A (2009) Elsevier

DOI: 10.1016/j.msea.2009.05.068

Microstructural and Micromechanical Characterisation of TiAl Alloys Using Atomic Force Microscopy and Nanoindentation

S. Gebhard [a, *], F. Pyczak [b], M. Göken

University of Erlangen-Nürnberg, Department of Materials Science and Engineering, General Materials Properties, 91058 Erlangen, Germany

[a] now at Institute of Materials Research, German Aerospace Centre (DLR), 51147 Cologne, Germany

[b] now at Institute for Materials Research, GKSS Research Centre Geesthacht, 21502 Geesthacht, Germany

Abstract

Different microstructures were generated in the Ti-45Al-4.6Nb-0.2B-0.2C and Ti-45Al-1Cr alloys (at.%) by heat treatment. The microstructures were investigated using nanoindentation and atomic force microscopy which was compared with transmission electron microscopy. Topographic contrast is usually used for phase identification in the atomic force microscope. However, it was found that the topographic order of the phases changes with different microstructures and specimen preparations. Nanoindentation measurements provided local hardness values not obtainable by other methods and enabled clear distinction of the phases. The hardness values can give information on surrounding microstructure and solid solution hardening. The mean lamellar spacing of the colonies was measured using both atomic force microscopy and transmission electron microscopy. Atomic force microscopy was found to be suitable to determine the spacing between α_2/γ-interfaces offering the advantages of easier sample preparation and fewer specimens compared to evaluation by TEM analysis.

Keywords: TiAl; Micromechanical properties; Nanoindentation; Atomic force microscopy

* Corresponding author. Tel. +49-2203-601-3139. Fax: +49-2203 696480. *E-mail address*: Susanne.Gebhard@dlr.de (S. Gebhard)

1 Introduction

In recent decades, research and development of TiAl alloys has focused on improving the mechanical properties for structural applications at high temperatures by optimising the microstructure [1-3]. It is well known that significant variations in mechanical properties can be obtained depending on the type of microstructure in γ-based titanium aluminide alloys [2,3]. The different microstructures can be generated by heat treatment and thermo-mechanical treatment, and the mechanical properties can be influenced accordingly. The mechanical properties are also influenced by alloying elements [4]. Niobium leads to a refinement of the microstructure [5], boron results in a small grain and colony size [6,7]. A finer microstructure exhibits higher strength in accordance with the well established Hall-Petch relationship [5,8,9]. The effect of other alloying elements, such as chromium and carbon, is an increase in ductility in the case of chromium [10] and an increase in hardness in the case of carbon. The latter is due to the formation of carbides [5].

In this work, the microstructures of a hot formed Ti-45Al-4.6Nb-0.2B-0.2C alloy and a cast Ti-45Al-1Cr alloy (at.%) were modified by different heat treatments and were investigated making use of an atomic force microscope (AFM). This method allows the study of very fine details of the microstructure on large samples without the need for intensive specimen preparation, as would be necessary for transmission electron microscopy (TEM). Atomic force microscopy in combination with nanoindentation yields information about local mechanical properties. The lateral resolution is less than one nanometre and mechanical properties of individual phase regions in highly refined microstructures can be measured. This work demonstrates that nanoindentation can also be used to identify phases by their different hardness values. Nanoindentation was previously applied to investigate the microstructure and local hardness of single phases

in polysynthetically twinned (PST) TiAl [11,12]. The present work shows that atomic force microscopy, especially when used in combination with nanoindentation, is a valuable tool for micromechanical and microstructural characterisation of polycrystalline TiAl alloys supplementing TEM and SEM.

2 Experimental Procedure

The materials used in this study were a hot formed Ti-45Al-4.6Nb-0.2B-0.2C (at.%) sheet and a cast and hot isostatically pressed ingot of Ti-45Al-1Cr (at.%). The sheet alloy showed a near-γ microstructure of fine globular γ-grains and small α_2-particles at the grain boundaries. The Ti-45Al-1Cr alloy had a fully lamellar microstructure in the as-received state.

The alloy composition has a strong influence on the phase diagram of TiAl alloys and additions of niobium are known to shift the α-transus temperature significantly [13]. Differential scanning calorimetry (DSC)-measurements were performed to get an idea of the temperatures for phase transformation in the investigated alloys. The Ti-45Al-4.6Nb-0.2B-0.2C alloy showed the α-transus at 1360 °C, the Ti-45Al-1Cr alloy possessed an α-transus temperature of 1374 °C.

Both alloys were heated up to a temperature of 1380 °C (above α-transus temperature of both alloys) and held at this temperature in a vacuum furnace for 15 minutes to modify the microstructures. One batch was subsequently furnace cooled (FC) at an initial cooling rate of about 15 $K(min)^{-1}$. Two other batches were cooled at constant rates of 1 $K(min)^{-1}$ and 0.5 $K(min)^{-1}$. To coarsen the microstructures of the as-received alloys they were annealed at 1180 °C for 24 h. The Ti-45Al-4.6Nb-0.2B-0.2C alloy was additionally heat treated at 1320 °C for 5 h to produce a duplex microstructure consisting of both γ-grains and lamellar colonies.

For AFM investigations, the samples were mechanically polished to 3 μm and further electrolytically polished using a solution of methanol, butanol and perchloric acid in a ratio of 0.6:0.34:0.06. This method is known to show a good contrast between the different intermetallic phases as well as between grains of the same phase [11,12]. A combination of a Berkovich indenter and an AFM was employed to measure the local hardness of the phases by nanoindentation. A loading force of 1500 μN was used for the hardness measurements. The hardness was evaluated from the load-displacement curves by the Oliver-Pharr method similar to the procedures used in [11,12].

Sample preparation for TEM included grinding the specimens to a thickness of 100 μm prior to electrolytic jet polishing with the same solution as that used for AFM preparation.

The mean lamellar spacing was measured from TEM micrographs taken with a Philips CM 200 transmission electron microscope. For comparison, the lamellar spacing of the microstructures was also determined using a Digital Instruments Dimension 3100 atomic force microscope. In TEM the lamellae were tilted 'edge-on' and about 200 lamellae from at least five colonies were considered. No distinction was made between γ/γ- and α_2/γ-interfaces. Similarly, in AFM all visible lamellae were included in the measurements. Since the colonies cannot be oriented in the AFM, only the colonies with lamellae thought to be perpendicular or nearly perpendicular to the surface were considered. This was ensured by only taking into consideration colonies whose average lamella width appeared to be minimal in the optical microscope of the AFM. Due to the fact that a typical specimen contained more than 200 grains, it was possible to select five or more grains with narrow lamella width for evaluation ensuring sufficiently good sampling.

3 Results and discussion

Microstructure investigation

Fig. 1 shows AFM images of the different investigated microstructures. In the as-received state of Ti-45Al-4.6Nb-0.2B-0.2C (Fig. 1a) and the coarsened near-γ microstructure (Fig. 1b, 1180 °C, 24 h) the γ-phase (depressed) and the α_2-phase (elevated) are easily identified as the morphology of the two phases is significantly different. Fig. 1c shows the duplex microstructure formed after 5 h at 1320 °C and furnace cooling. In this case, the grains, which are supposed to be γ-phase, appear elevated. However, the γ-phase was identified as the depressed phase in the AFM-micrographs of the near-γ microstructures. Fig. 1d shows a fully lamellar microstructure (15 min, 1380 °C, FC) with an apparent small border zone around the colonies. The border zone consists of the depressed phase. During cooling, the γ-lamellae form in an α- or α_2-matrix [14]. Since γ-plates nucleate preferentially at prior α-grain boundaries, it could be assumed that the border consists of γ-phase.

The Ti-45Al-1Cr alloy always exhibits a fully lamellar microstructure (Fig. 1e-h) and no near-γ or duplex microstructures could be obtained by heat treatment. However, other parameters, such as lamellar spacing and colony size, could be influenced by changing the heat treatment parameters. Most colony boundaries showed no border zone in the Ti-45Al-1Cr alloy, as visible in the as-received state (Fig. 1e) and the coarsened state after 24 h at 1180 °C (Fig. 1f). With respect to the identification of the phases γ and α_2 in the AFM, it is interesting to note that the fully lamellar microstructure shown in Fig. 1g (1380°C, 15 min, FC) possesses a border zone around the different colonies consisting of a phase which appears to be elevated.

Phase identification

AFM scans of different grains and lamellae in the near-γ, duplex and lamellar microstructures of the Ti-45Al-4.6Nb-0.2B-0.2C alloy after nanoindentation are shown in Fig. 2. Different indent sizes produced with the same load correspond to variations of the local hardness. The higher the hardness of a material the smaller are the resulting indents. Previous measurements on PST-crystals showed that the α_2-phase is the harder one of the two phases [11]. In the near-γ microstructure (Fig. 2a) the phase sticking out of the surface is the α_2-phase showing smaller indents than the depressed γ-phase. However, the size of the indents in the duplex microstructure (Fig. 2b) as well as in the fully lamellar microstructure (Fig. 2c) indicates clearly that the γ-phase is the elevated one and not the α_2-phase. This is especially obvious considering the duplex microstructure, which contains both γ-grains and lamellar colonies. Similar results were obtained in the lamellar microstructures of the Ti-45Al-1Cr alloy.

A possible reason for the inversion of the topographic contrast is a different response of the α_2-phase and the γ-phase when preparing different microstructures of TiAl alloys with electrolytic polishing. This could be caused by internal stresses, particularly coherency stresses. PST-TiAl crystals studied with atomic force microscopy are reported to show a topography similar to the one found in the globular microstructures observed in this work (i.e. elevated α_2-phase and depressed γ-phase) [11,12]. Therefore, chemical composition and varying local crystal orientation might influence the electrolytic polishing process as well. Other preparation methods like solely mechanical polishing might prevent this contrast inversion phenomenon. Nevertheless, when characterizing TiAl-microstructures solely by AFM one should be aware of this problem.

Local hardness measurements

Hardness measurements using a nanoindenting AFM (NI-AFM) were performed on all microstructures to gain further information about the mechanical properties of the different phases. Fig. 3 shows typical load-displacement curves obtained using a NI-AFM on different grains and particles of a near-γ microstructure of the Ti-45Al-4.6Nb-0.2B-0.2C alloy. The α_2-phase has a higher hardness than the γ-phase, which is also obvious when comparing the different indentation depths for the same force of 1500 μN. For the α_2-phase a hardness between 7.6 and 9.5 GPa was obtained in all investigated microstructures of this alloy. The hardness of the γ-phase varied between 4.4 to 6.0 GPa. The Ti-45Al-1Cr alloy showed a slightly lower hardness of 6.8 to 8.0 GPa for the α_2-phase and a hardness of 4.4 to 5.5 GPa for the γ-phase. The results obtained in this work depend on the respective microstructure under investigation. Considering the lamellar microstructures in Ti-45Al-4.6Nb-0.2B-0.2C and Ti-45Al-1Cr, it is obvious that a decreasing lamellar spacing (given as λ near the respective hardness value of the γ-phase in Fig. 4) results in a higher hardness. This is in agreement with a hardening of the Hall-Petch type if we assume that the indentation with a maximum force of 1500 μN results in indentation depths, where the influence of nearby interfaces on the measured hardness cannot be ignored in the relatively fine lamellar microstructures. Comparing the two near-γ microstructures and the γ-grains in the duplex microstructure of the Ti-45Al-4.6Nb-0.2B-0.2C alloy, one would expect either to find no difference in hardness, or to find an increase in hardness with decreasing grain size (given as *d* near the respective hardness value of the γ-phase in Fig. 4). The latter would be the case if even in these relatively coarse microstructures the hardness was influenced by internal interfaces (i.e. grain boundaries). However, the lowest

hardness is measured in the coarsened near-γ microstructure and the duplex microstructure, which also exhibits the smallest grain size. Since there is no consistent way to explain the measured differences in hardness by the grain size, they are most probably caused by the plastic pre-deformation in the as-received microstructure which was produced by rolling. The hardness measured in the γ-grains in the duplex microstructure and the coarsened near-γ microstructure is assumed to be the "pure" hardness of the γ-phase of the Ti-45Al-4.6Nb-0.2B-0.2C alloy, excluding any influences of plastic pre-deformation and constraints by grain or lamellar boundaries. Remarkably**,** it is approximately equal to the hardness in the coarsest lamellar microstructure of the Ti-45Al-1Cr alloy. If one assumes that in these specimens neither confinement of dislocation movement by nearby interfaces, nor plastic pre-deformation influences the hardness, one must expect that the main factor governing the hardness is a difference in alloy composition. It was reported by Appel et al. that niobium does not have a significant solid solution hardening effect but refines the microstructure [5]. Appel et al. came to this conclusion indirectly from the results of creep experiments. The present results are from direct measurements. They support this conclusion when one takes into consideration that chromium produces no significant solid solution hardening either [3].

In addition, varying the orientations of the indented particles and grains influences the hardness. This becomes obvious when comparing the load-displacement curves measured on differently oriented γ-grains of the Ti-45Al-4.6Nb-0.2B-0.2C alloy (Fig. 3). However, the different orientations influence the hardness to a much lesser degree than the different microstructures.

Different orientations are indicated by differences in the shape of pile-ups around the indents (Fig. 5). Depending on the plastic anisotropy of the phases [12], the pile-ups show different shapes (see the long drawn-out form of the pile-ups in Fig. 5a compared

to the more compact shape of the pile-ups in Fig. 5b) and can appear on one, on two or on all sides of the indent. Even though the load-displacement curves of the α_2-phase show hardly any variation, the investigated particles must have had different orientations, too. However, the pile-ups in the α_2-phase were not as distinct as in the γ-phase.

We confine our discussion of the hardness differences in the various microstructures of the two alloys to the γ-phase as it is uncertain if the variation in the hardness measured in the very fine α_2-particles and lamellae is really an effect of the microstructure or of measurement problems in such fine phases (e.g. impression of the α_2-particle in the underlying softer γ-phase). With respect to this it should also be mentioned that the average hardness values for the α_2-phase given above may be systematically too low due to such effects.

Nevertheless, this tool gives valuable information about the local mechanical properties and the difference in hardness of the two phases. In combination with direct imaging of the indented phase by a NI-AFM it makes distinct phase identification possible.

Comparison of AFM and TEM measurements of the lamellar spacing

Due to its excellent lateral resolution the AFM offers the possibility to study very fine details of the microstructure, such as the lamellar spacing, which are usually investigated by TEM. Fig. 6 shows the dependence of the lamellar spacing on the cooling rate for both alloys, which can be described by a power law [15,16]. The slopes shown in Fig. 6 depend on the alloy under investigation and on the microscope used for the measurement.

In the TEM micrographs a slope of -0.6 was observed in the Ti-45Al-4.6Nb-0.2B-0.2C alloy and a slope of -0.4 was observed in the Ti-45Al-1Cr alloy. These results are in the

same range as those reported by Beschliesser et al. [7], who found a slope of -0.39, and Takeyama et al. [16], who observed a slope of -0.5. Beschliesser et al. attributed the difference between their results and the results of Takeyama et al. to the different alloy composition and the fact that Takeyama et al. only counted the α_2/γ-interfaces while they counted both the α_2/γ- and the γ/γ-interfaces. In the present study, no distinction was made between the α_2/γ- and the γ/γ-interfaces and both were counted if visible when evaluating the TEM and AFM micrographs. The Ti-45Al-4.6Nb-0.2B-0.2C alloy mainly showed α_2/γ-interfaces. The fully lamellar microstructure of the Ti-45Al-1Cr alloy possessed high fractions of both types of interfaces. The different slopes of the two alloys could be due to the different alloy compositions and / or the different character of lamellar interfaces.

The AFM measurements result in the same slope of -0.6 for both alloys. It is assumed that the AFM measurements provide equal results for both alloys because they mainly evaluate the distance of the α_2/γ-interfaces. Due to the poorer contrast of the γ/γ-interfaces compared to the strong contrast of the α_2/γ-interfaces in the AFM no distinction of adjacent γ-lamellae could be made. This is especially true if a scan size is chosen which is big enough to give a good sampling of the lamellar spacing in one colony (around 50 to 100 lamellae). The AFM results are in accordance with the TEM results if the α_2/γ-interfaces are the majority of lamellar boundaries present in the specimen (Ti-45Al-4.6Nb-0.2B-0.2C). In this case, the lamellar spacing and the distance between the α_2/γ-interfaces are almost equal. For this reason, the different slopes of the TEM results could be caused by the different types of lamellar boundaries included in the evaluation rather than by the different chemical composition of the two alloys.

It is understandable that niobium does not significantly affect the distance between the α_2/γ-interfaces in the Ti-45Al-4.6Nb-0.2B-0.2C alloy compared with Ti-45Al-1Cr (same slope for AFM-measurements in both alloys) since niobium partitions nearly equally between the γ- and α_2-phases. Thus, no strong redistribution of niobium is necessary if α_2/γ-interfaces move during lamella growth. The distribution of niobium was measured by energy dispersive spectroscopy (EDS) in the TEM. The niobium content in the γ-phase varied from 3.8 to 5.5 at.% and from 4.0 to 5.5 at.% in the α_2-phase at different measurement positions. This is in good agreement with results published by Liu et al. [8].

The good agreement between AFM and TEM results achieved for the Ti-45Al-4.6Nb-0.2B-0.2C alloy indicates that the error caused by the inability to ascertain edge-on orientation of the lamellae during AFM measurements is small as long as the contrast between the lamellae is good enough to observe all existing lamellae and as long as the colonies whose lamellae are thought to be perpendicular or almost perpendicular are the only ones chosen for the investigation. Therefore, the AFM is found to be suitable for measuring the lamellar spacing. It has the advantage of being less time consuming and much easier in preparation compared to TEM measurements. The AFM also provides the opportunity to study a greater area and accordingly, the number of specimens required for analysis can be significantly reduced. With respect to SEM, which also benefits from easier specimen preparation compared to TEM, NI-AFM has the advantage of providing additional information about local mechanical properties.

4 Conclusions

- Phase identification using a NI-AFM shows that the topography of the phases can change if electrolytic polishing is performed. Nanoindentation can be used to identify the phases clearly and, additionally, measure the mechanical properties.
- NI-AFM measurements show that the α_2-phase is significantly harder than the γ-phase in both alloys.
- The hardness differences of the γ-phase in different microstructures can be related to a Hall-Petch hardening in finer microstructures and plastic pre-deformation introduced during processing. In agreement with other work no evidence for significant solid solution hardening of niobium could be found.
- Due to the poor contrast of the γ/γ-interfaces in the AFM lamellar distances measured from AFM micrographs are representative of the α_2/γ-interface distance.
- Atomic force microscopy proved to be a suitable method for the investigation of the microstructures usually encountered in TiAl-alloys. It supplements the well established methods of SEM and TEM. Even though the lamellae could not be tilted into an edge-on orientation in the AFM, the results obtained for the spacing between α_2/γ-interfaces from TEM analysis and AFM analysis are in good agreement.

5 Acknowledgements

We want to thank Dr. H. Kestler from Plansee AG and Prof. Dr. B. von Großmann from Audi AG for providing the TiAl alloys.

6 Literature

[1] Y. W. Kim, Journal of Metals 41 (1989) 24.

[2] Y. W. Kim, Journal of Metals 43 (1991) 40.

[3] Y. W. Kim, Journal of Metals 46 (1994) 30.

[4] S.-C. Huang in: R. Darolia, J. J. Lewandowski, C. T. Liu. P. L. Martin, D. B. Miracle, M. V. Nathal (eds.), Structural Intermetallics, TMS, Warrendale, PA, 1993. p. 299.

[5] F. Appel, M. Oehring, R. Wagner, Intermetallics 8 (2000) 1283.

[6] M. E. Hyman, C. McCullough, C. G. Levi, R. Mehrabian, Metall. Trans. 22 A (1991) 1647.

[7] M. Beschliesser, A. Chatterjee, A. Lorich, W. Knabl, H. Kestler, G. Dehm, H. Clemens, Mat. Sci. Eng. A 329-331 (2002) 124.

[8] Z. C. Liu, J. P. Lin, S. J. Li, G. L. Chen, Intermetallics 10 (2002) 653.

[9] Y. W. Kim, Intermetallics 6 (1998) 623.

[10] T. Kawabata, T. Tamura, O. Izumi in: C.T. Liu, A.I. Taub, N.S. Stroloff, C.C. Koch (eds.), High Temperature Ordered Intermetallic Alloys III, MRS, Pittsburgh, 1989, p. 329.

[11] M. Göken, M. Kempf, W. D. Nix, Acta Mater. 49 (2001) 903.

[12] M. Kempf, M. Göken, H. Vehoff, Mat. Sci. Eng. A 329-331 (2002) 184.

[13] W. J. Zhang, G. L. Chen, F. Appel, in: D.G. Morris, S. Naka, P. Caron (eds.), Intermetallics and Superalloys, Proc. EUROMAT 1999, Wiley-VHC, Weinheim, 1999, p. 362.

[14] Y. Yamabe, M. Takeyama, M. Kikuchi, in: Y. W. Kim, R. Wagner, M. Yamaguchi, Gamma Titanium Aluminides, TMS, Warrendale, PA, 1995, p.112.

[15] Y. W. Kim, D.M. Dimiduk in: M. V. Nathal, R. Darolia, C. T. Liu, P. L. Martin, D. B. Miracle, R. Wagner, M. Yamaguchi (eds.), Structural Intermetallics (1997) 531.

[16] M. Takeyama, T. Kumagai, M. Nakamura, M. Kikuchi in:

R. Darolia, J. J. Lewandowski, C. T. Liu, P. L. Martin, D. B. Miracle, M. V. Nathal (eds.), Structural Intermetallics, TMS, Warrendale, PA, 1993, p. 167.

Figure Captions

Fig. 1. Microstructures of the Ti-45Al-4.6Nb-0.2B-0.2C alloy: (a) as-received, (b) near-γ (1180 °C, 24 h, FC), (c) duplex (1320 °C, 5 h, FC), (d) fully lamellar (1380 °C, 0.25 h, FC), and of the Ti-45Al-1Cr alloy: (e) as-received, (f) coarsened (1180 °C, 24 h, FC), (g) fine lamellar (1380 °C, 0.25 h, FC) and (h) coarse lamellar (1380 °C, 0.25 h, 0.5 $K(min)^{-1}$).

Fig. 2. Near-γ microstructure (a), duplex microstructure (b) and fully lamellar microstructure (c) of the Ti-45Al-4.6Nb-0.2B-0.2C alloy with nanoindents in the different phases.

Fig. 3. Load-displacement-curves of the α_2- and γ-phases taken from the coarsened near-γ microstructure of the Ti-45Al-4.6Nb-0.2B-0.2C alloy.

Fig. 4. Hardness values of the γ-phase of the Ti-45Al-1Cr alloy (grey) and the Ti-45Al-4.6Nb-0.2B-0.2C alloy (white) taken from different microstructures. The lamellar spacing λ and the grain size d are given.

Fig. 5. Pile-ups around the nanoindents in two γ-grains of the coarsened near-γ microstructure of the Ti-45Al-5Nb-0.2B-0.2C alloy indicating different crystal orientations.

Fig. 6. Comparison of the AFM- and TEM-measurements of the Ti-45Al-1Cr alloy (a) and the Ti-45Al-4.6Nb-0.2B-0.2C alloy (b).

Figure 1a

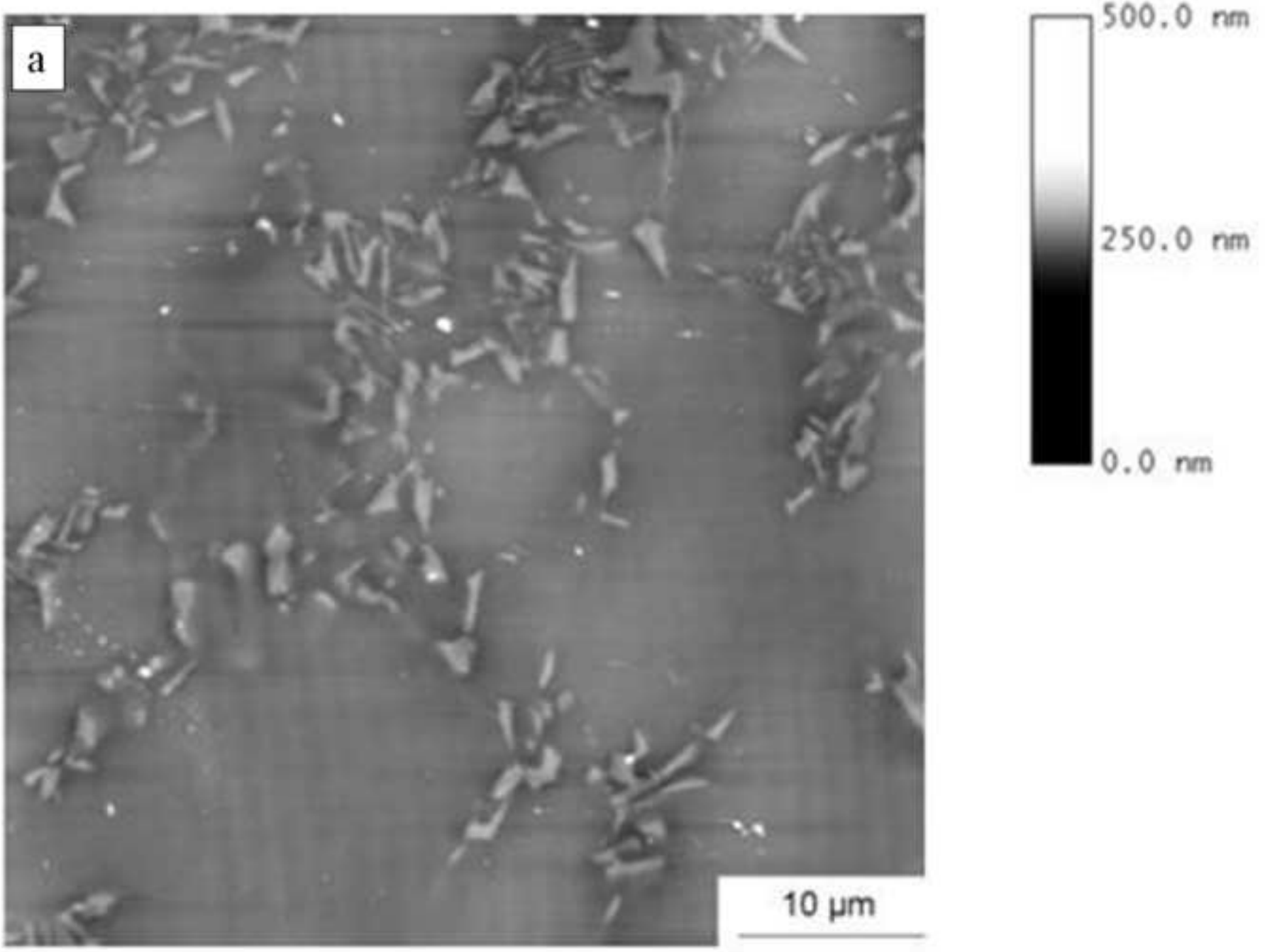

Figure 1b

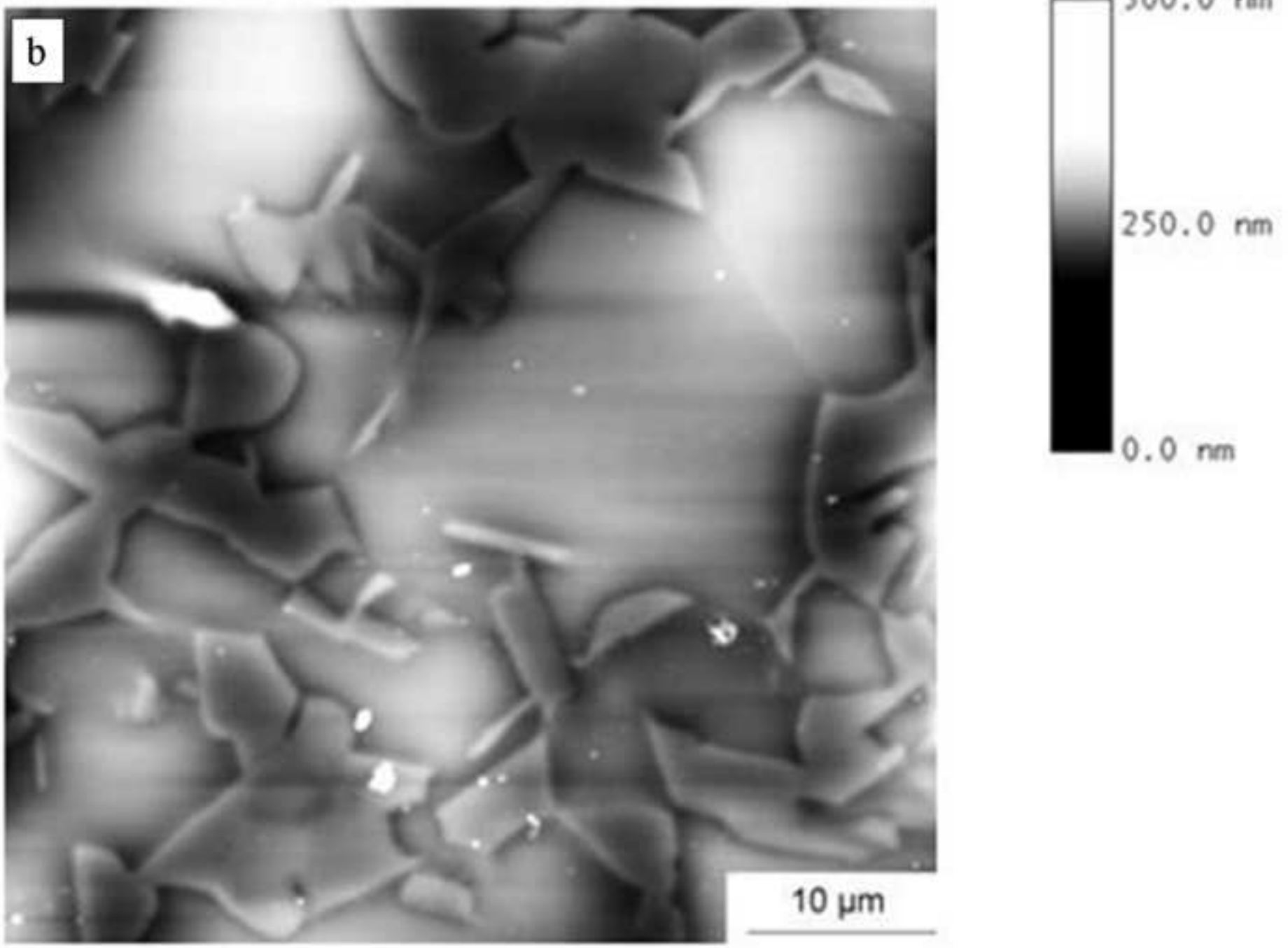

Figure 1c

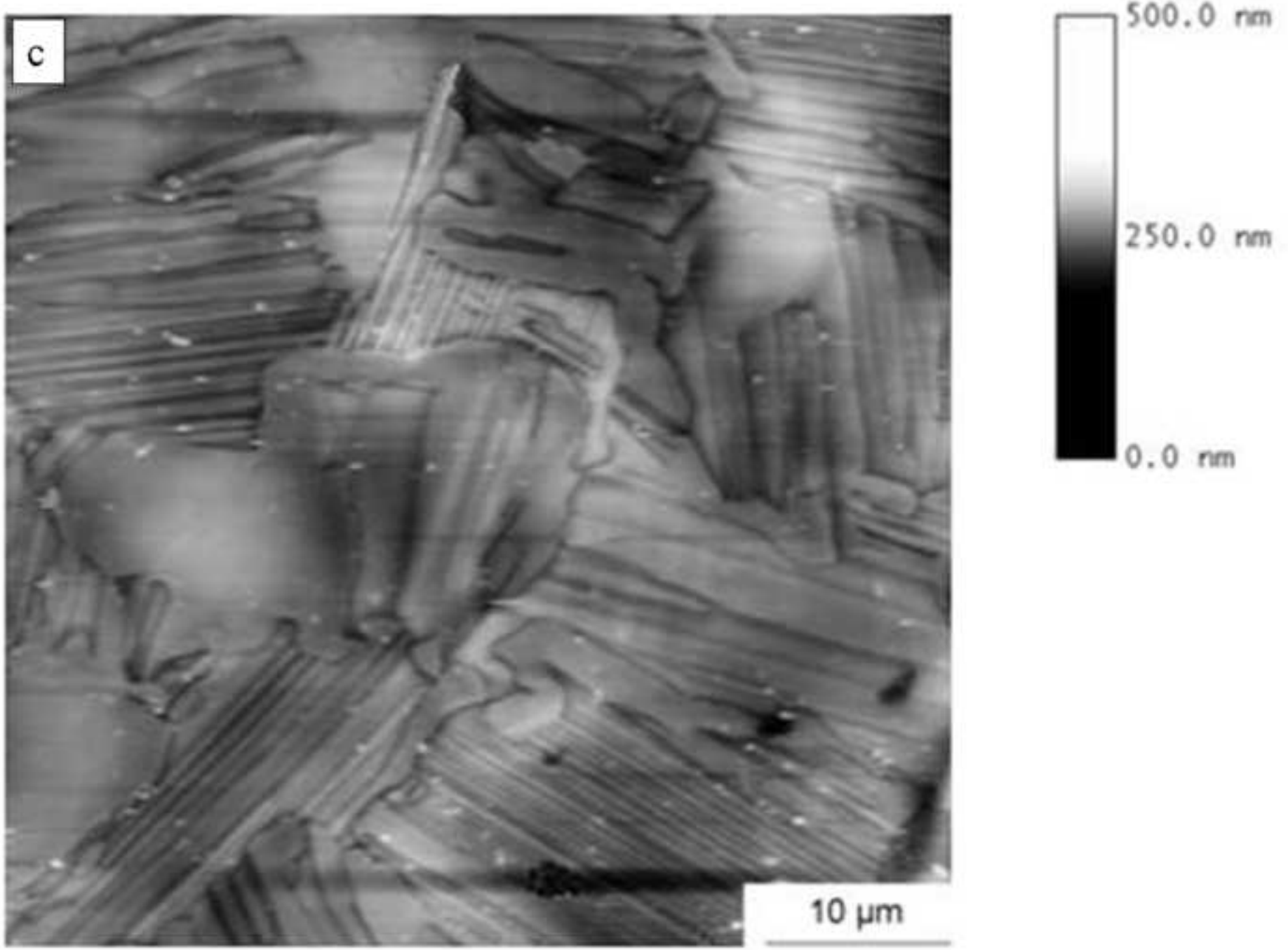

Figure 1d

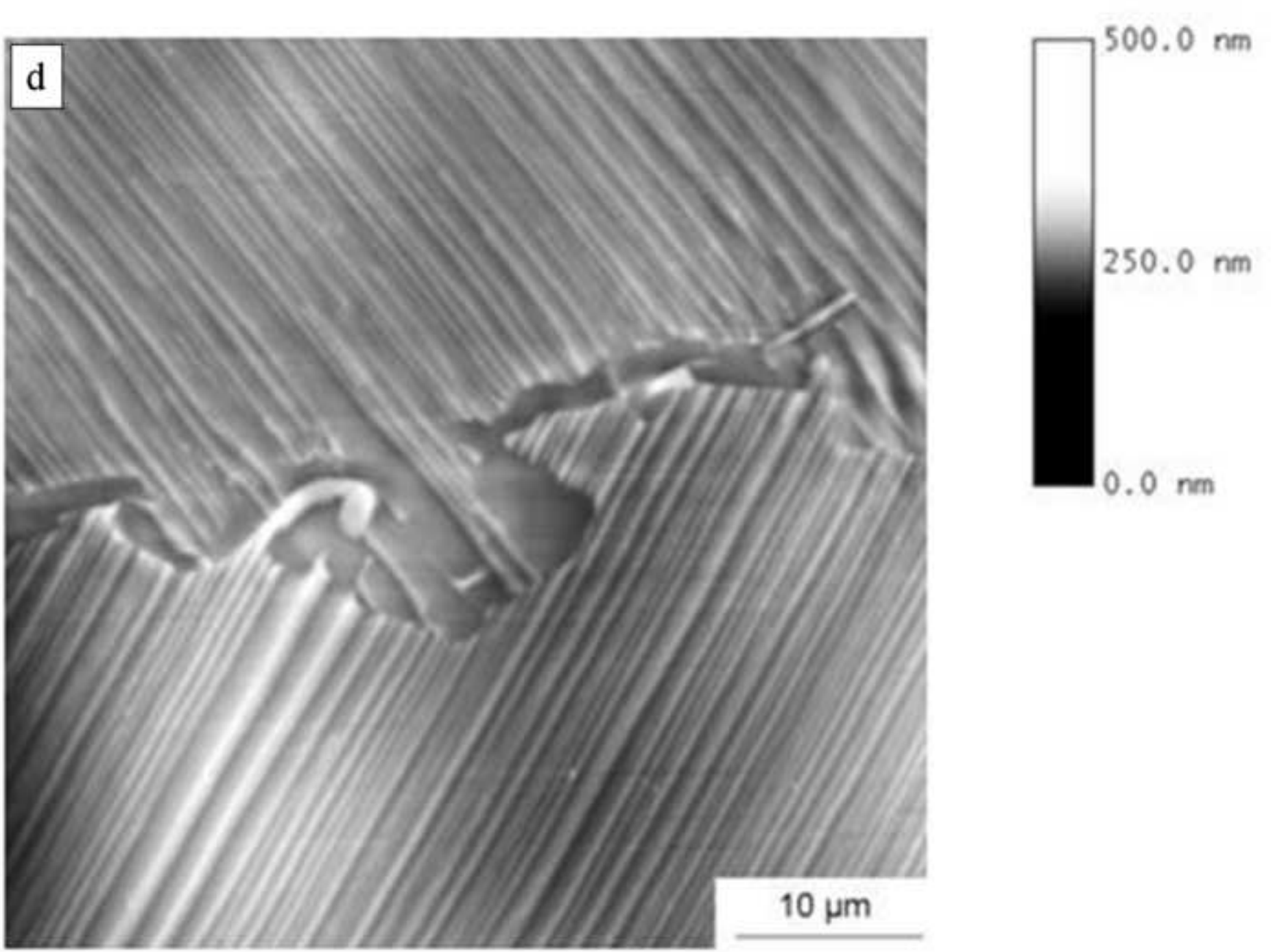

Figure 1e

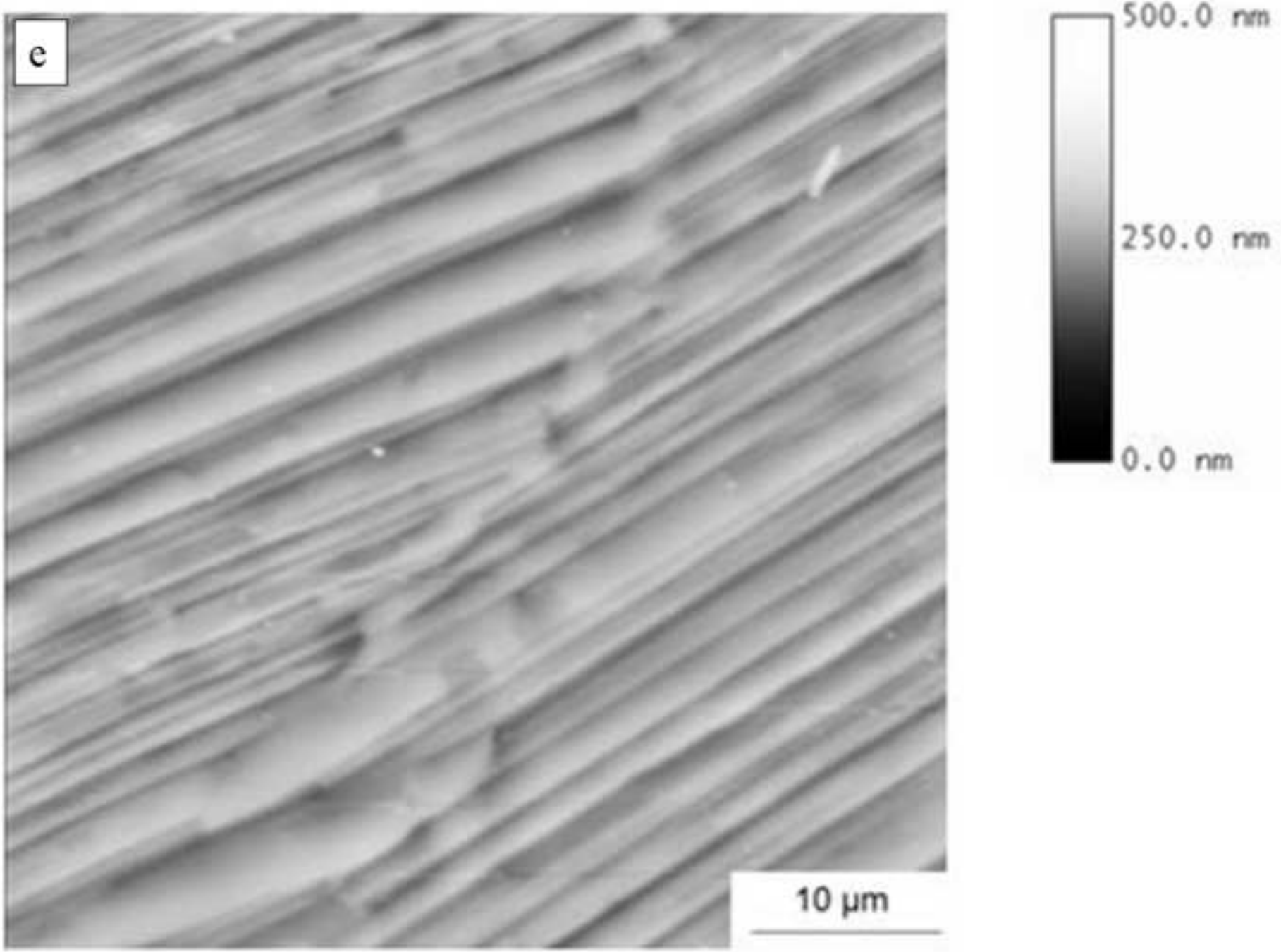

Figure 1f

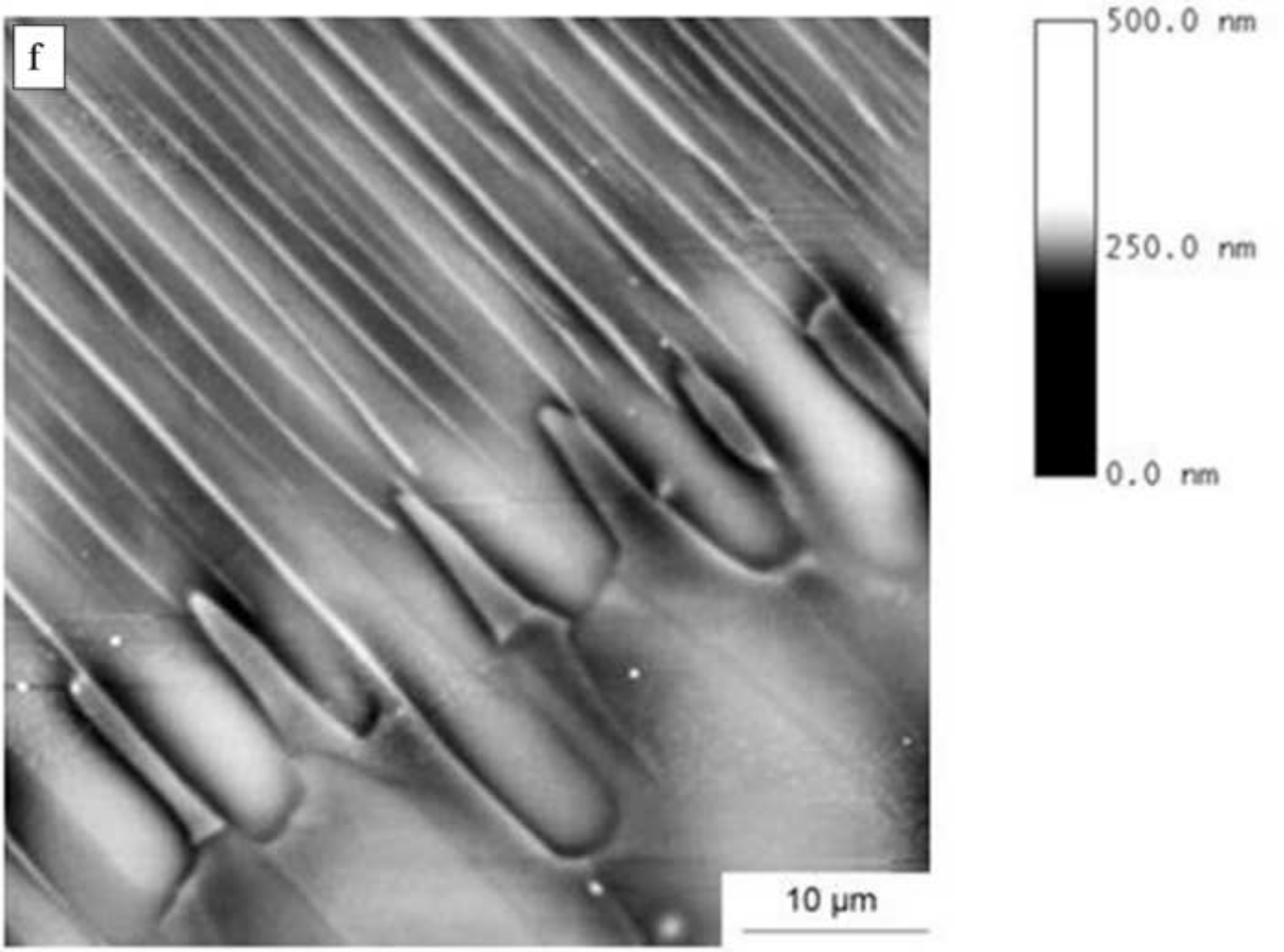

Figure 1g

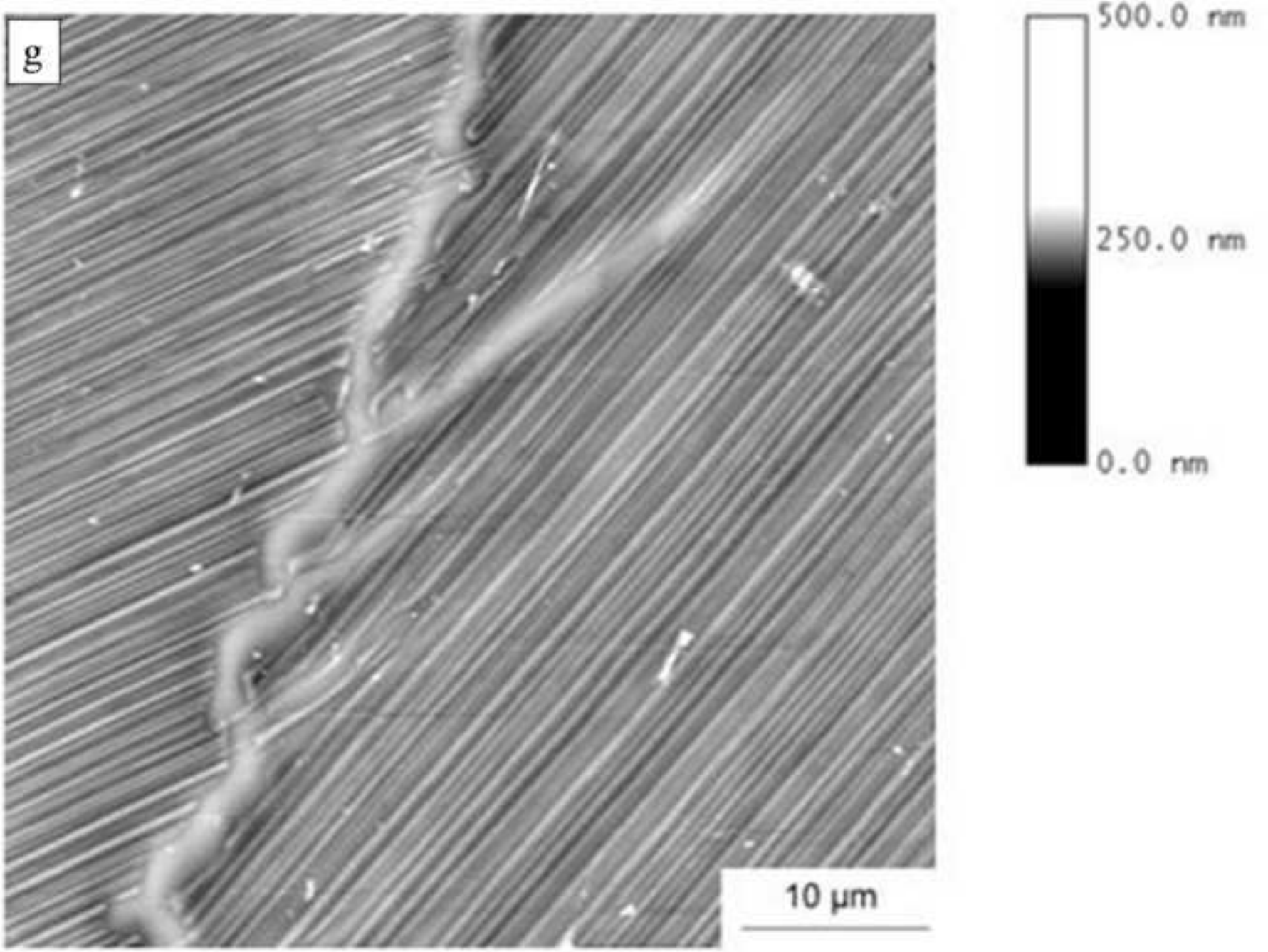

Figure 1h

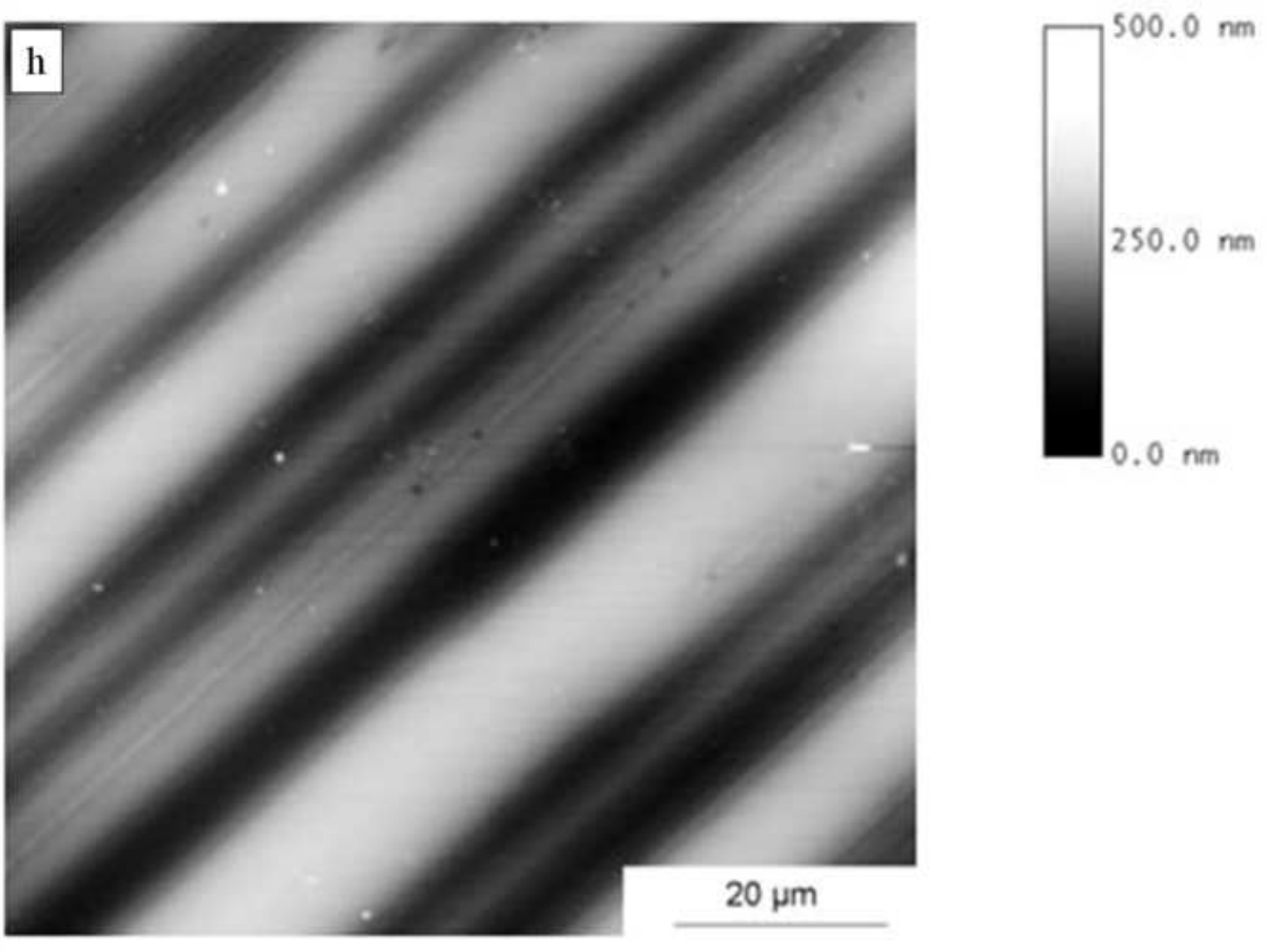

Figure 2a

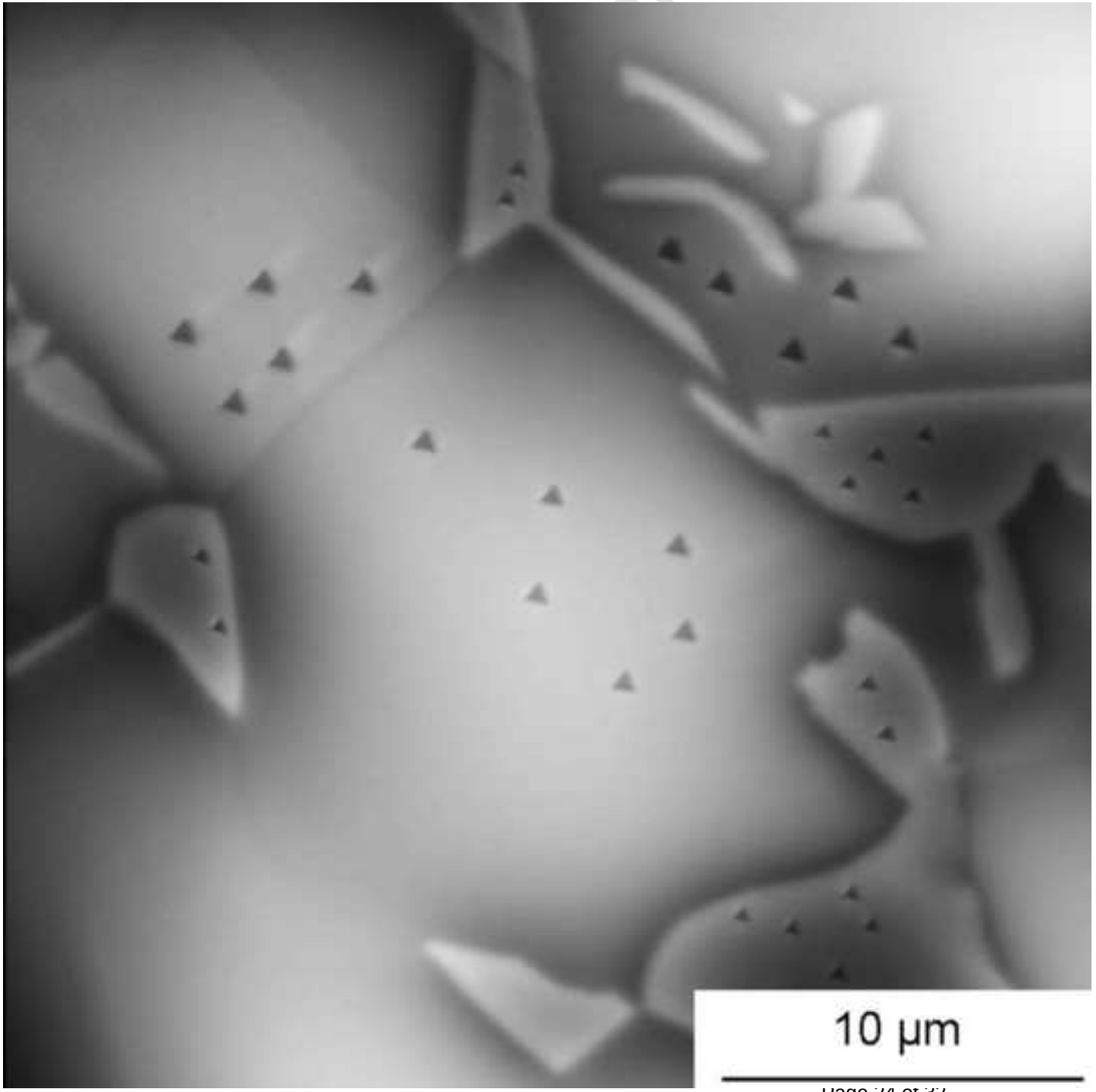

Figure 2b

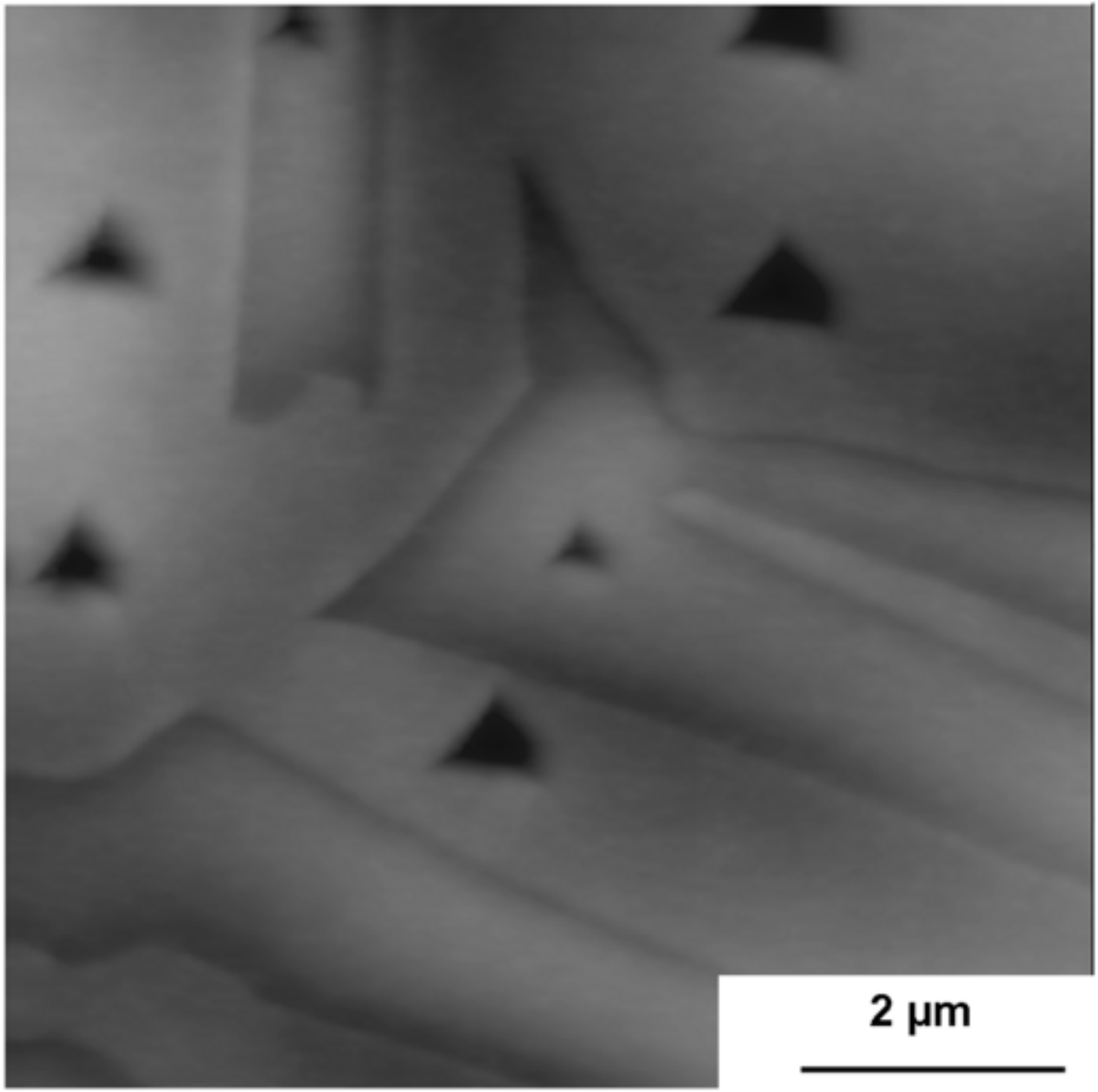

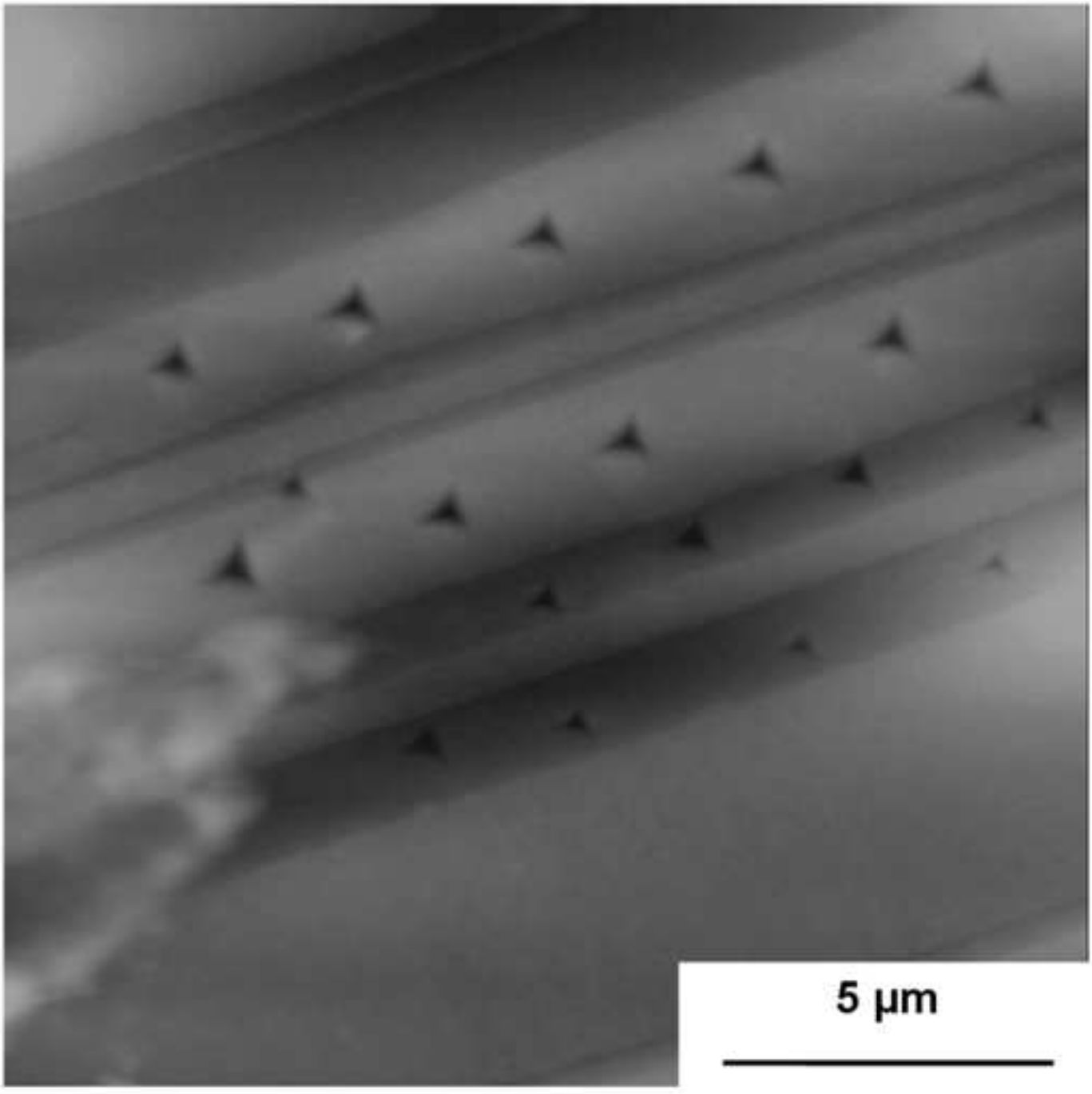

Figure 3

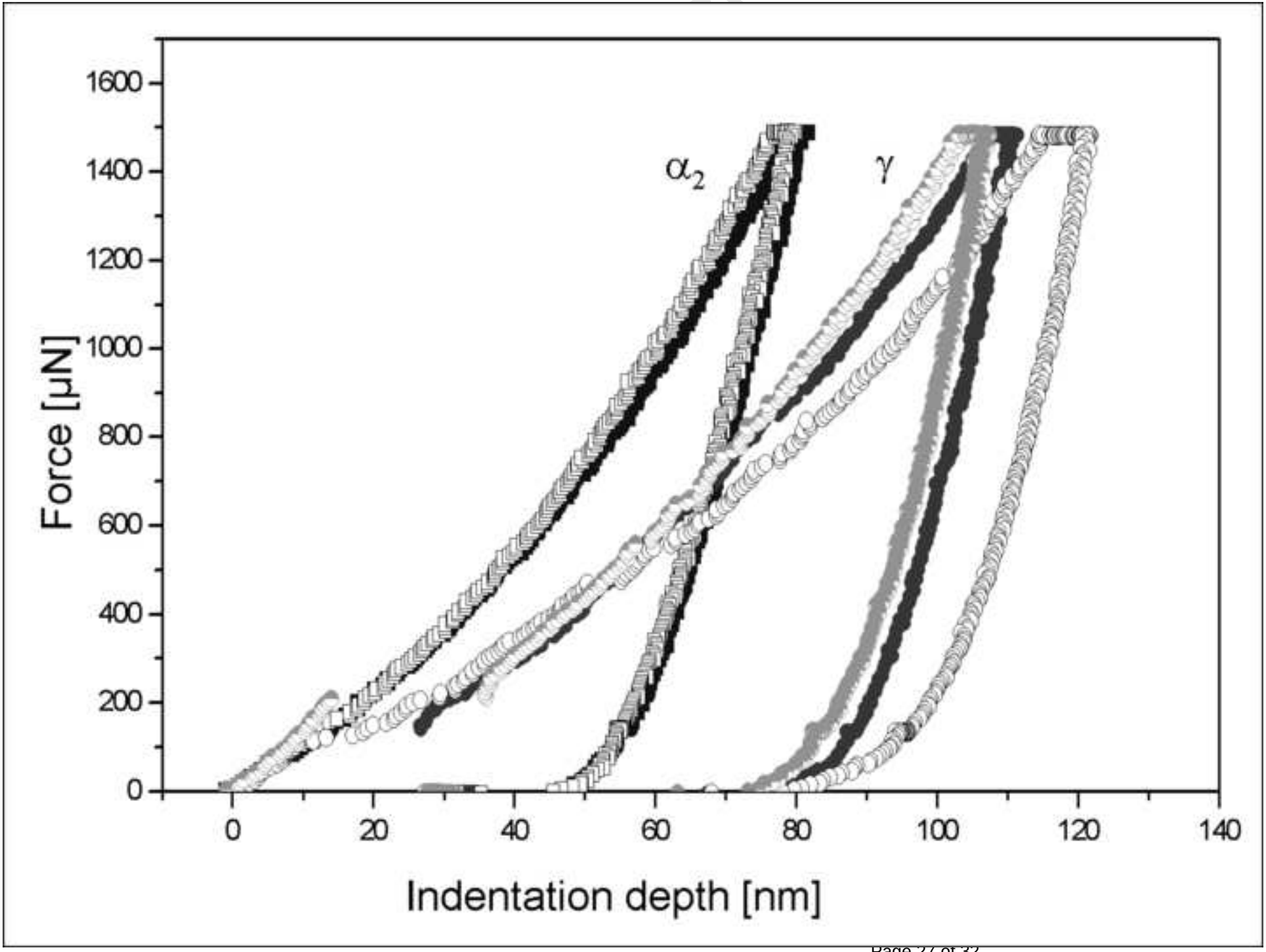
1600
1400
1200
1000
800
600
400
200
0
Force [μN]
0
20
40
60
80
100
120
140
Indentation depth [nm]
α2
γ

Figure 4

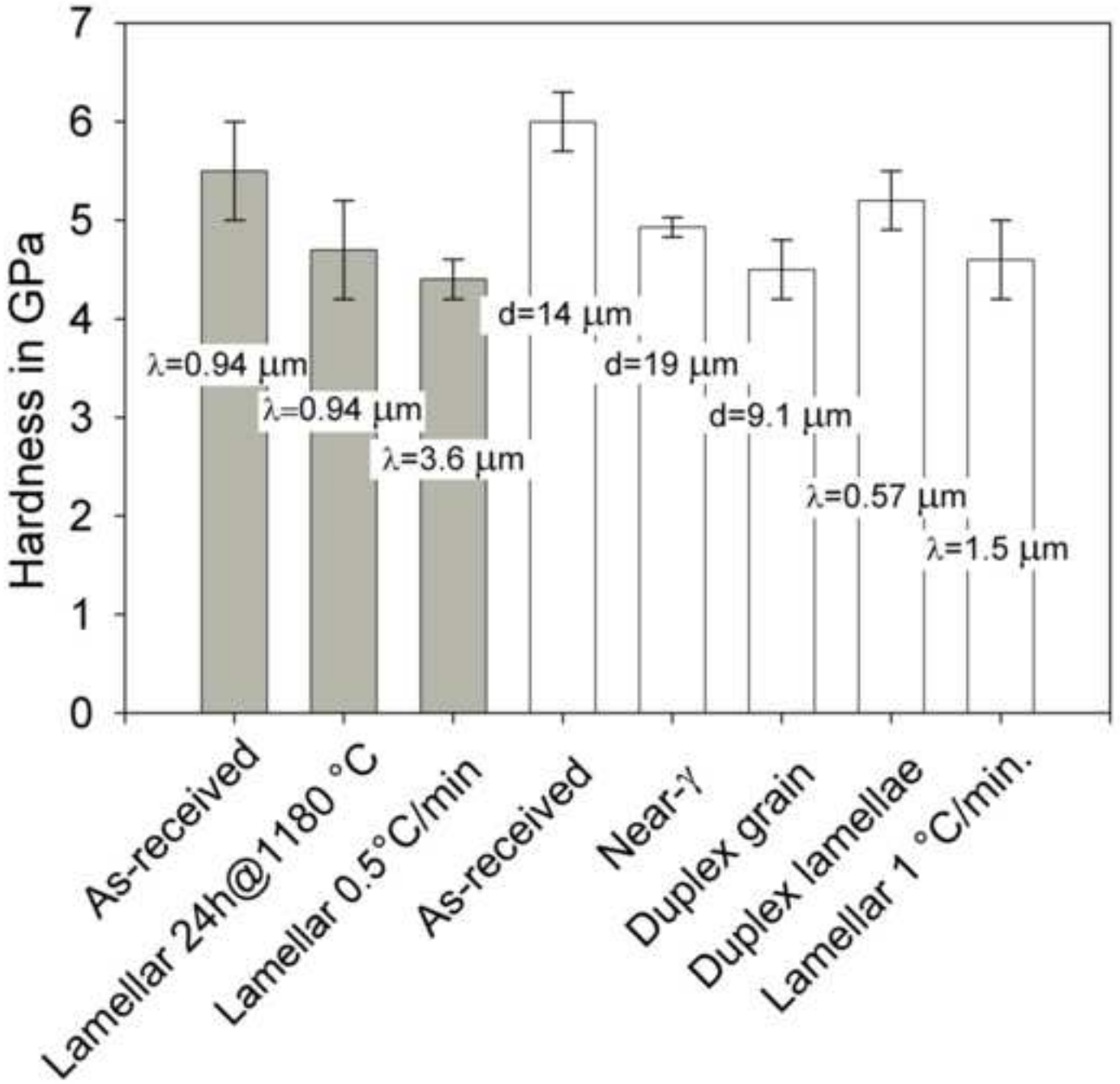
Hardness in GPa
0
1
2
3
4
5
6
7
λ=0.94 μm
λ=0.94 μm
λ=3.6 μm
d=14 μm
d=19 μm
d=9.1 μm
λ=0.57 μm
λ=1.5 μm
As-received
Lamellar 24h@1180 °C
Lamellar 0.5°C/min
As-received
Near-γ
Duplex grain
Duplex lamellae
Lamellar 1 °C/min.

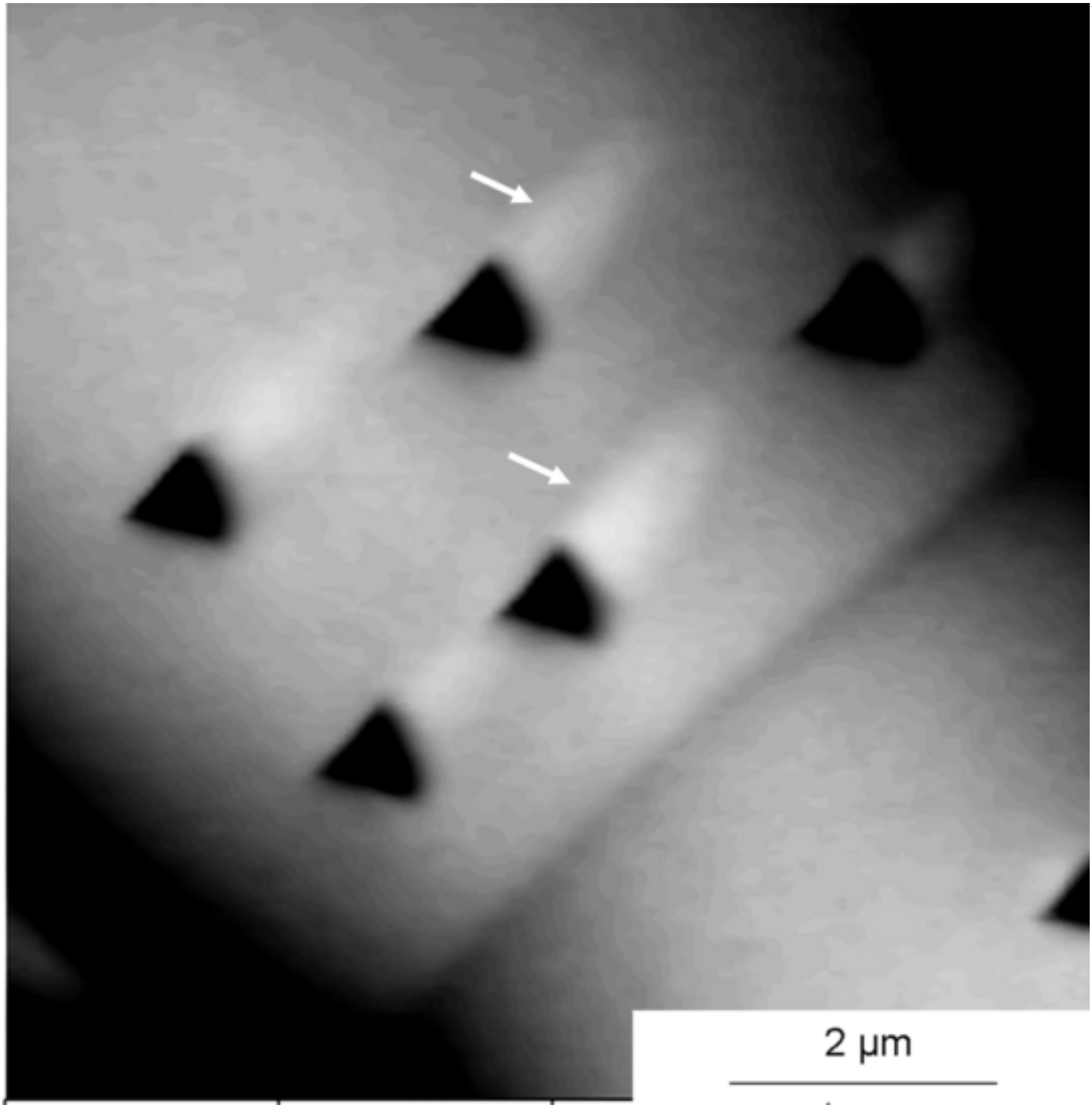

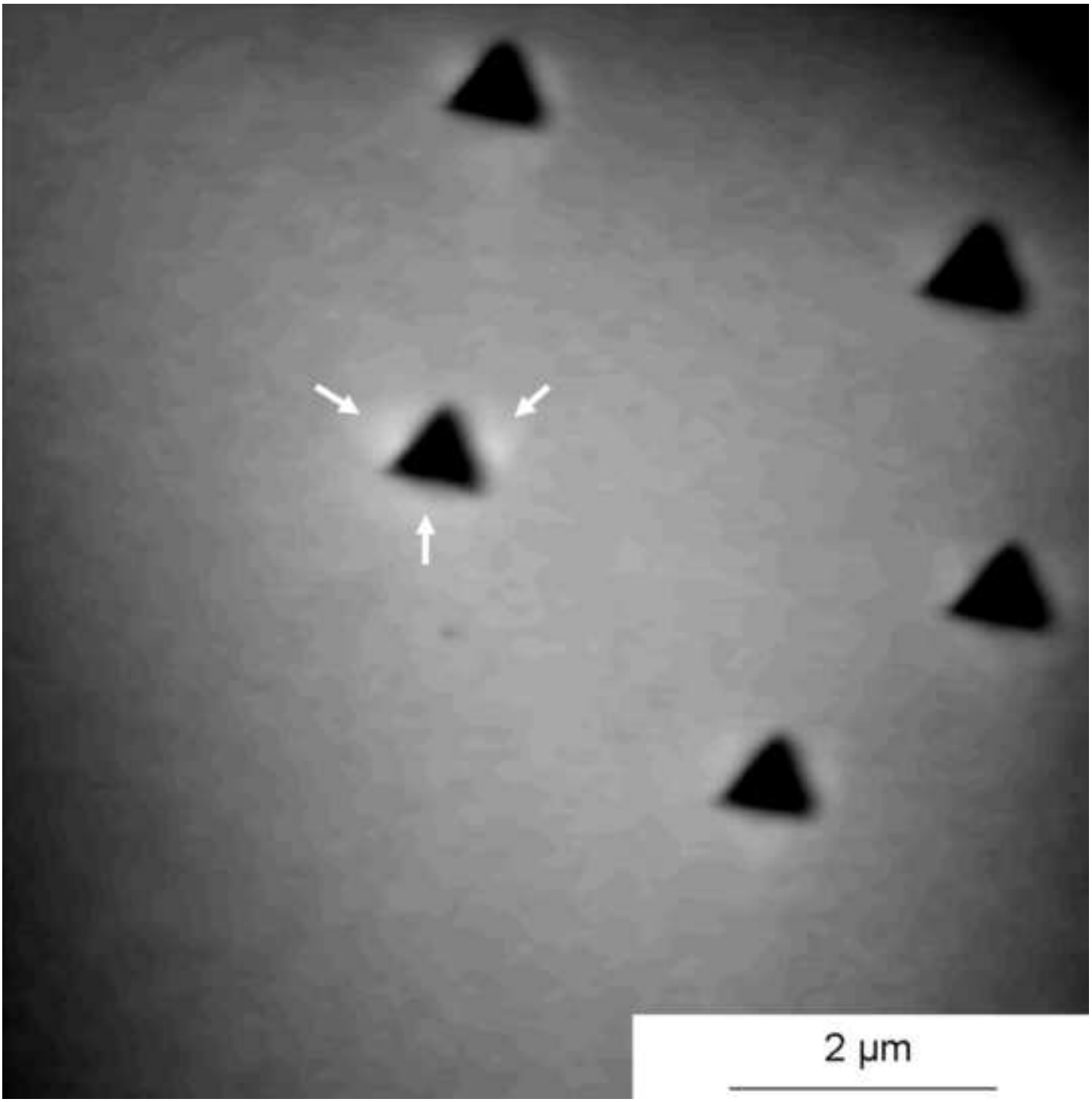

Figure 6a

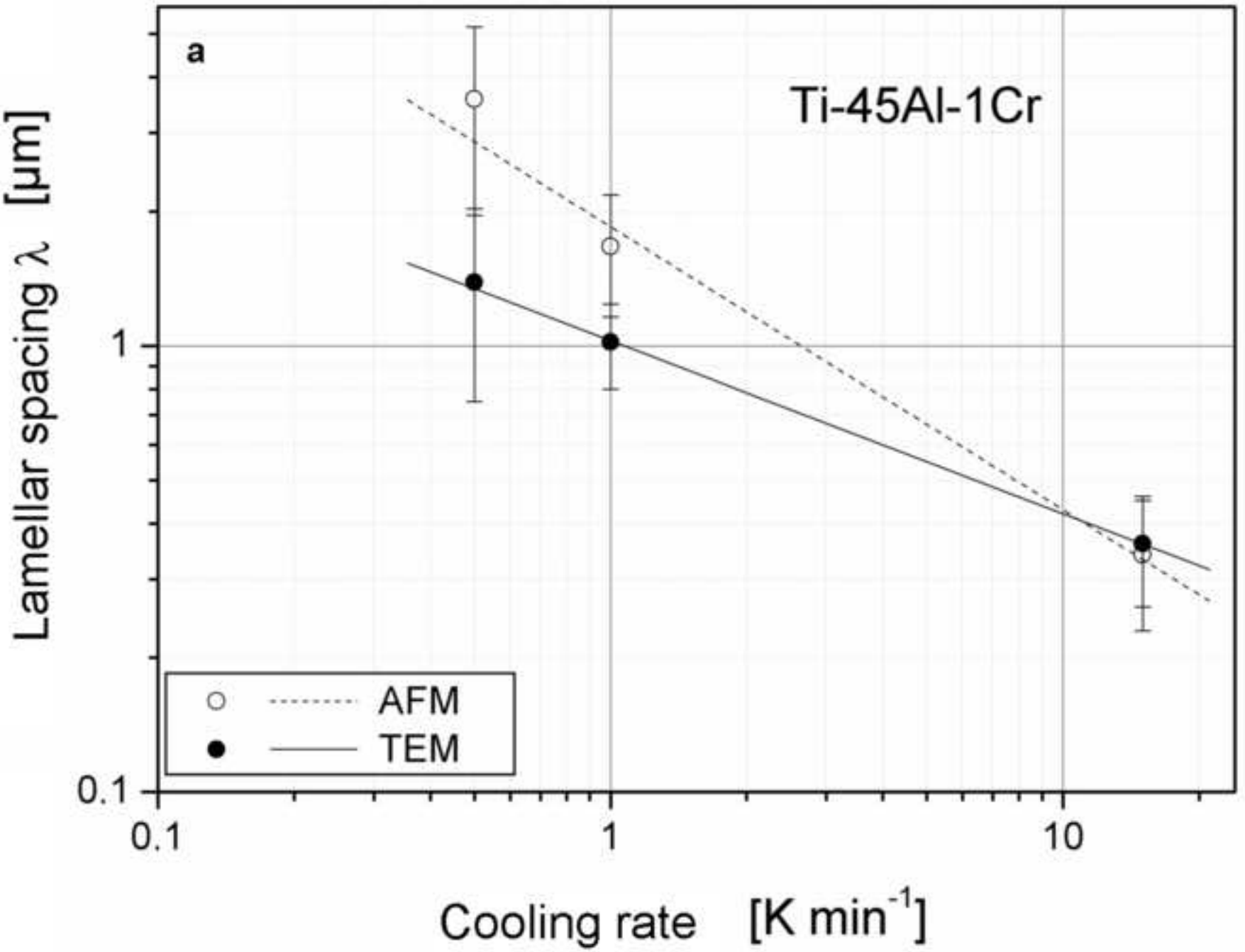
a
Ti-45Al-1Cr
Lamellar spacing λ [μm]
1
0.1
0.1
1
10
Cooling rate [K min-1]
AFM
TEM

Figure 6b

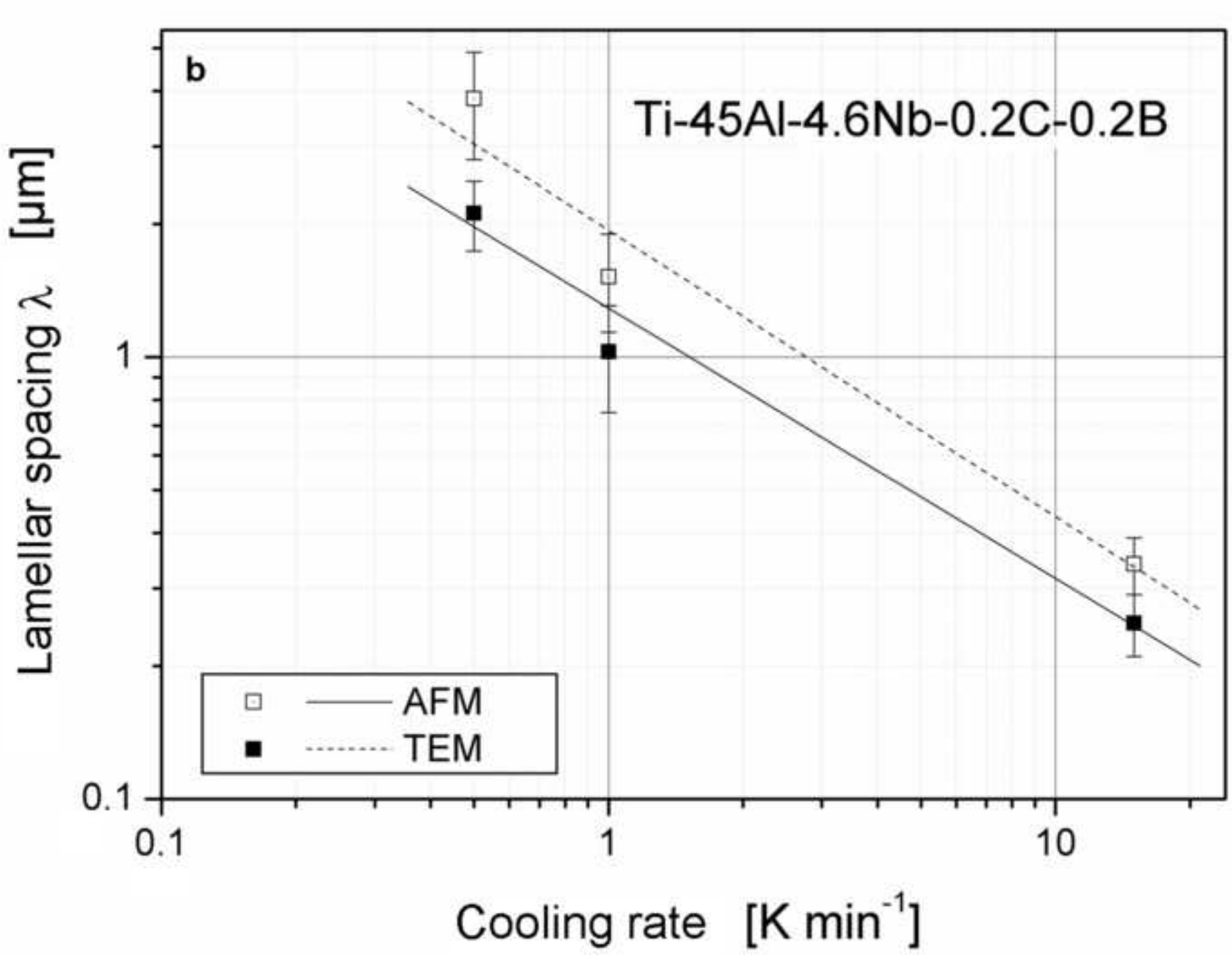
b
Ti-45Al-4.6Nb-0.2C-0.2B
Lamellar spacing λ [µm]
1
0.1
0.1
1
10
Cooling rate [K min-1]
AFM
TEM